JOURNAL OF
POWER
SOURCES

Electrodeposited Ni–Sn intermetallic electrodes for advanced lithium ion batteries

J. Hassoun, S. Panero, B. Scrosati *

Department of Chemistry, University of Rome "La Sapienza", 00185 Rome, Italy

Abstract

Various samples of Ni_xSn_y metallic alloys electrodeposited under different current and time regimes have been prepared and tested in lithium cells. The results clearly demonstrate that the electrochemical performance of these intermetallic electrodes greatly depends on the synthesis conditions which in turn reflect on the type of morphology and phase of the various samples. The best electrode cycled with a high capacity delivery, i.e. of the order of $550\,mA\,hg^{-1}$ and showed an efficient behaviour when used as anode in a lithium ion battery using $LiNi_{0.5}Mn_{1.5}O_4$ as cathode. These results confirm that the electrodeposition is a very promising synthesis tool for monitoring the morphological and phase conditions of Ni_xSn_y and that the approach described in this work may be used for further optimizing this intermetallic electrode.
© 2006 Elsevier B.V. All rights reserved.

Keywords: Lithium alloy; Intermetallic; Ni–Sn; Anode; Lithium ion battery

1. Introduction

Lithium metal alloys, LiM, have received large attention in the lithium ion battery R&D. Indeed, these materials have a very high specific capacity and, due to these properties, they are considered as very appealing negatives electrodes to exploited in replacement of conventional graphite in advanced design, lithium ion batteries. Indeed, large research efforts are presently devoted to this class of materials and many types of them have been prepared and characterized [1–5]. However, these materials suffer of large volume expansion and contraction during the charge–discharge cycling and this induces mechanical disintegration which in turn results in a very poor cycle life.

A way to solve this problem is to move to M_1M_2 intermetallics where the electrochemical process in a lithium cell involves the displacement of one metal M_2 which forms the lithium alloy LiM_2 while the other metal M_1 acts as an electrochemically inactive matrix to buffer the volume variations during the alloying process. Among others, tin-based intermetallics have received a particular attention [6] due to their specific properties which combine high charge storage with low cost. Various

compositions have been investigated to identify the ones which are the most promising in terms of battery applications. The Ni_3Sn_4 is one of these [7–10].

However, even under the intermetallic configuration, the capacity retention of the electrode is not satisfactory upon prolonged cycling. Clearly, the morphology of the intermetallic plays a key role, especially in terms of particle size and of interparticle space, for achieving a proper control of the stress associated to the volume changes. Accordingly, the choice and the optimization of a proper preparation method becomes an essential factor for achieving good electrode performance.

Various methods are commonly used to prepare the lithium alloys. They include ball milling [10] and sol–gel precipitation [11]. However, the synthesis route which is the most suitable to control the final morphology of the desired intermetallic electrode is electroplating since. Indeed, by changing the current regimes and/or the type of substrate, one can easily modulate the form of and the size of the electrodeposited material. The benefit of this type of synthesis was already stressed by Mukaibo et al. [8] and in this work we have further refined the study by using a different approach. Mukaibo et al. have focused on the role of the composition of the electroplating solution [8] while in this work we have evidenced the role of the electrodeposition parameters by comparing the electrochemical performances of various samples of Ni_3Sn_4 electrodeposited on a copper foil

* Corresponding author.
E-mail address: bruno.scrosati@uniroma1.it (B. Scrosati).

under different current and time conditions. Accordingly, the main purpose of this work is the definition of these parameters with the aim of providing useful information on the characteristics of the electrodeposition process.

2. Experimental

The Ni_3Sn_4 samples were obtained by electrodeposition on a copper foil in a two-electrode glass cell. An aqueous solution similar to that recommended by Mukaibo et al. [8], i.e. formed by $NiCl_2$ 0.075 M, $SnCl_2$ 0.175 M, $K_4P_2O_7$ 0.5 M, glycine 0.125 M and NH_4OH 5 ml l^{-1}, was used as the electrolyte and a Pt foil as the counter electrode. The electrodeposition current and time conditions were monitored using a Maccor Series 4000 Battery Test System.

The structure of the samples was controlled by XRD, using a Rigaku X-ray diffractometer miniflex and their morphology by scanning electron microscopy, SEM, using SEM-EDS Leo 1450 VP.

The electrochemical response of the samples was tested in a cell formed by the following sequence: (i) an electrode formed by the given Ni_3Sn_4 sample electrodeposited on a copper foil (which acted as current collector), (ii) a 1 M $LiPF_6$ solution in an ethylene carbonate–dimethyl carbonate, EC:DMC 1:1 (Merck Battery Grade) electrolyte soaked on a Whatman^{TM} separator and (iii) a lithium metal foil electrode. The electrochemical response of this cell was monitored by a Maccor Series 4000 Battery Test System.

The lithium ion cell was formed by using the selected Ni_3Sn_4 sample as anode, the quoted 1 M $LiPF_6$ EC:DMC 1:1 solution as electrolyte and a $LiNi_{0.5}Mn_{1.5}O_4$ as cathode. The latter was deposited as a thin film on an aluminium substrate by doctor-blade deposition of a slurry composed of 80% $LiNi_{0.5}Mn_{1.5}O_4$ (active material), 10% PVdF 6020, Solvay Solef (binder) and 10% SP carbon (electronic support). The cell was cycled at 0.5 A cm^{-2} g^{-1} and under 3.0–4.8 voltage limits, using a Maccor Series 4000 Battery Test System as the controlling instrument.

3. Results and discussion

In order to investigate the role of the synthesis conditions in affecting the electrochemical properties of the final product, we have prepared six Ni_3Sn_4 samples electrodeposited under different current and time regimes, keeping the charge at the value of 1.8 C cm^{-2}. The preparation conditions of these samples are summarized in Table 1 while Fig. 1 reports in comparison the samples' weight obtained under the various applied conditions. As expected, by increasing the deposition current, the losses progressively increase with an associated decrease of the amount of the electrodeposited material.

First, XRD was used to check the structural characteristics of the six samples. Fig. 2 shows the evolution of the diffraction spectra passing from sample NiSn-1 to sample NiSn-6. As expected for samples prepared for electrodeposition [8,12], the peaks of all samples can be ascribed both to the Ni_3Sn_4 phase and to the Ni_xSn_y metastable phase. From literature data [8,11], this metastable phase can be reported as a mixture of Ni_3Sn, Ni_3Sn_2,

Table 1
Electrodeposition parameters of the Ni_3Sn_4 samples investigated in this work

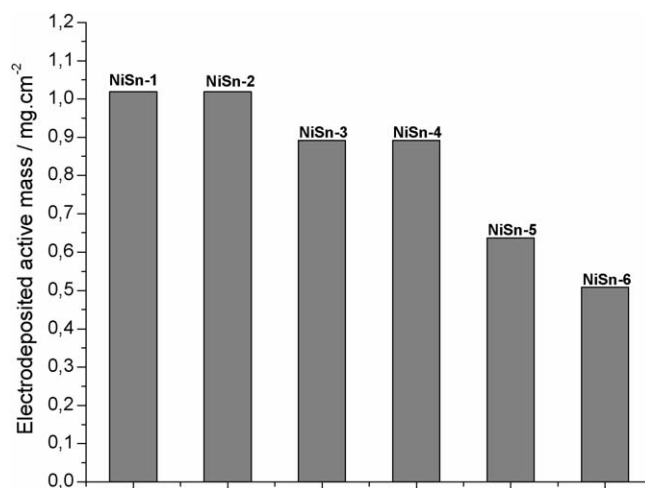| Sample	Electrodeposition current (mA cm^{-2})	Electrodeposition time (min)
NiSn-1	0.5	60
NiSn-2	1.0	30
NiSn-3	2.0	15
NiSn-4	3.0	10
NiSn-5	6.0	5
NiSn-6	15	2

Fig. 1. Amount of electrodeposited materials for the various Ni_3Sn_4 samples prepared through electrodeposition on a Cu foil at different current density/time conditions. Total deposition charge: 1.8 C cm^{-2}.

Ni_4Sn and $NiSn_2$ phases. The Ni_3Sn_4 phase is predominant in samples NiSn-1, NiSn-2, NiSn-6 and the combined metastable phase Ni_xSn_y for samples NiSn-3, NiSn-4 and NiSn-5. The main difference is in the crystallinity of the samples which increases passing from sample NiSn-1 to sample NiSn-4, to decrease again moving to samples NiSn-5 and NiSn-6.
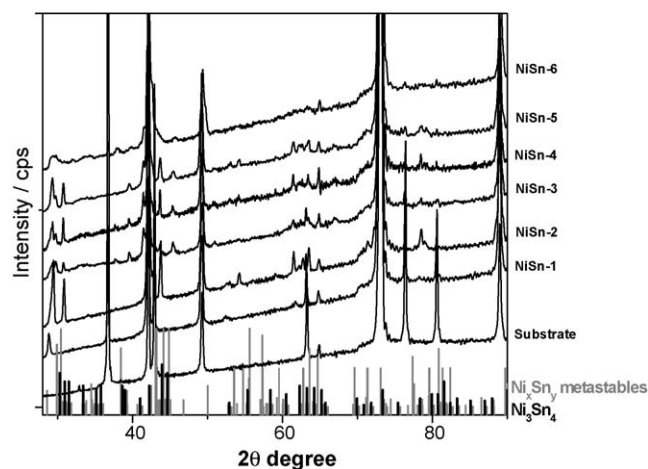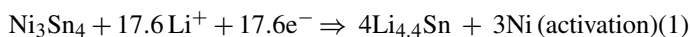

Fig. 2. XRD patterns of the various Ni_3Sn_4 samples prepared through electrodeposition on a Cu foil at different current density/time conditions. For samples' identification see Table 1.

These XRD results provide a preliminary indication that indeed the conditions of electrodeposition may greatly affect the characteristics of the samples. This is further confirmed by the SEM investigation. Fig. 3A–F show in comparison the morphology of the various electrodeposited samples. Substantial differences among the samples can be observed. Sample NiSn-1 has a compact, cauliflower-like morphology consisting in pillars formed by aggregates of small grains, Fig. 3A. However, this morphology progressively changes for the samples electrodeposited at increasing current values. In the case of sample NiSn-2 pores start to develop on the top of the pillars, Fig. 3B, and this porosity becomes more extended in sample NiSn-3, Fig. 3C. Moving to samples electrodeposited at high current regimes, the morphology return compact with the progressive growth of the pillars, see Fig. 3D and E and with a change in the size of the grains, see Fig. 3F.
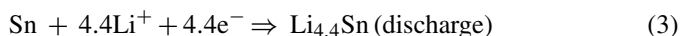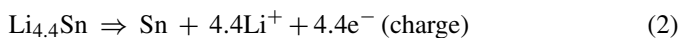
These difference in morphology are expected to reflect in differences in the electrochemical behaviour. This has been verified by examining the cycling response of the various samples in a lithium cell. It is assumed that the electrochemical process is that generally expected for the M_1M_2 intermetallics, which, in the specific case of the material here investigated, can be written as:

First cycle:

$$Ni_3Sn_4 + 17.6\,Li^+ + 17.6e^- \Rightarrow 4Li_{4.4}Sn + 3Ni\,(activation) \quad (1)$$

Following cycles:

$$Li_{4.4}Sn \Rightarrow Sn + 4.4Li^+ + 4.4e^-\,(charge) \quad (2)$$

$$Sn + 4.4Li^+ + 4.4e^- \Rightarrow Li_{4.4}Sn\,(discharge) \quad (3)$$

While the first cycle is irreversible, the following ones are reversible and represent the steady state electrochemical operation of the electrode to which is associated a total, theoretical capacity of 993 mA hg^{-1}, calculated on the basis of process [3].

Fig. 4 reports the capacity delivered upon discharge (see process [3]) when cycling samples NiSn-1, NiSn-2, NiSn-3, NiSn-4, NiSn-5 and NiSn-6, respectively, as the positive electrode in a
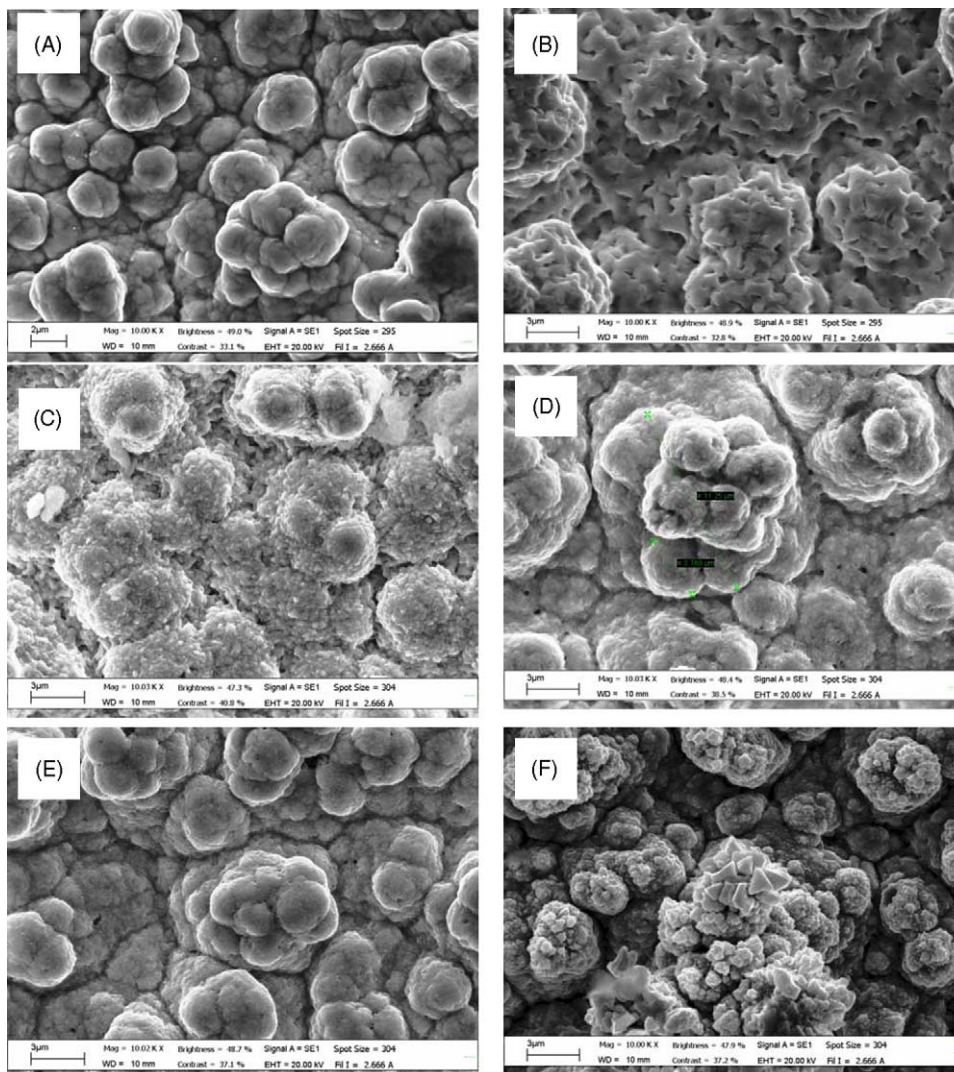

Fig. 3. SEM images of the various Ni_3Sn_4 samples investigated in this work: NiSn-1 (A); NiSn-2 (B); NiSn-3 (C); NiSn-4 (D); NiSn-5 (E) and NiSn-6 (F). For samples' identification see Table 1.
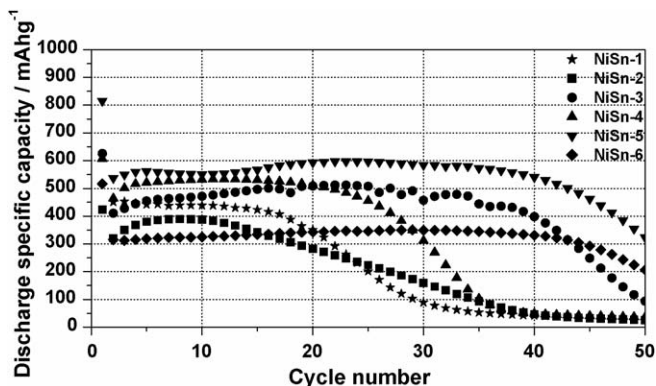
Fig. 4. Discharge capacity delivered upon cycling of lithium cells using samples NiSn-1, NiSn-2, NiSn-3, NiSn-4, NiSn-5 and NiSn-6, respectively, as cathode. EC:DMC 1:1 LiPF$_6$ electrolyte. Charge–discharge current density: 1 A cm^{-2} g^{-1}, about 0.8C rate. Room temperature. For samples' identification see Table 1.

lithium cell. Fig. 5 shows the respective voltage profiles at the 10th cycle.

Important information can be obtained by examining Fig. 4. First we notice an initial decay in capacity when passing from the first to the following cycles. This can be associated to the ongoing of the first activation cycle, see Ref. [1], which is irreversible. This indirectly supports the suggested overall electrochemical process as written above. The decay in capacity vanishes in the following cycles which evolve with a high charge–discharge efficiency, see Fig. 5. In this steady state regime, the cells operate in charge and in discharge according to processes [2] and [3], respectively, which are reversible.

However, there is a dramatic difference among the value and the stability of the capacity delivered by the various cells. Clearly, cells based on cathode samples where the metastable Ni$_x$Sn$_y$ phase is predominant, i.e. samples e NiSn-3, NiSn-4 and NiSn-5, have the highest capacity, i.e. ranging from 450 to 550 mA hg^{-1}. These values represent 45 and 55%, respectively, of the theoretical capacity, assuming the complete ongoing of the

process [1]. These are very good percentage of capacity, especially considering the high rate at which the cycles are run, i.e. 0.8C. On the contrary, cells based on the other samples have either low stability, see cells with samples NiSn-1 and NiSn-2, respectively, or a low delivered capacity, see cell with sample NiSn-6.

These are typical results which confirm that the type of the predominant phase and of the related morphology, and thus, the conditions of the synthesis, play a definite role in affecting the electrochemical performance of the intermetallic electrodes. From Fig. 6 which summarizes the performance of the cells in terms of capacity delivered at the 50th cycle, we see that the electrode based on sample NiSn-5 largely outperforms all the other electrodes. Thus, one may conclude that the best synthesis conditions for electrodeposited materials to be proposed as electrodes in lithium cells, are those which imply a relatively high current for a limited time, in order to obtain an uneven deposition, however, still maintaining a certain degree of regularity. The SEM Fig. 3E shows that the morphology of the sample prepared under these conditions, i.e. sample NiSn-5, is based on pillars formed by a regular agglomeration of low particle size grains. This partial regularity vanishes in part when passing to samples obtained under more drastic conditions in terms of electrodeposition current, as it is the case of sample NiSn-6. Indeed, from Fig. 3F, which illustrates the morphology of this sample, one can clearly notice that the pillars collapse. In addition, the size of the deposited grains appears to progressively increase, although this effect needs to be confirmed. Accordingly, the electrochemical performance decays, see Fig. 4. Probably, this decay is associated to the increase in the particle size and to the decrease in the degree of porosity. Passing from sample NiSn-5 to sample NiSn-6 there is also a change in the predominant phase which is metastable for the former and the Ni$_3$Sn$_4$ for the latter, see Fig. 2. To be recalled that the metastable phase is assumed to have a Ni:Sn composition ratio of almost 1:1 with Ni melted into Sn [8]. Obviously, this particular structure assures a favourable condition for an efficient evolution of the electrochemical process, as demonstrated by the experimental results of Fig. 4 which
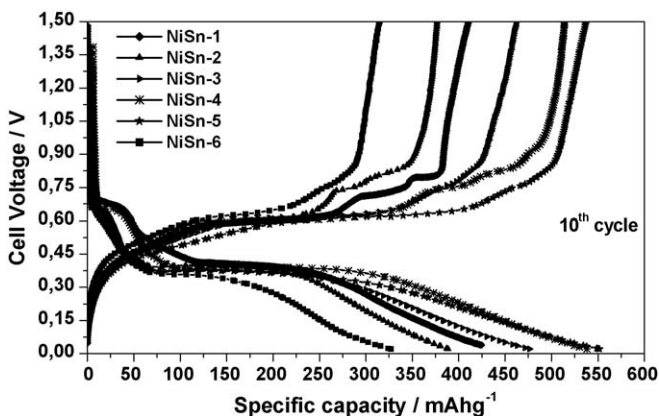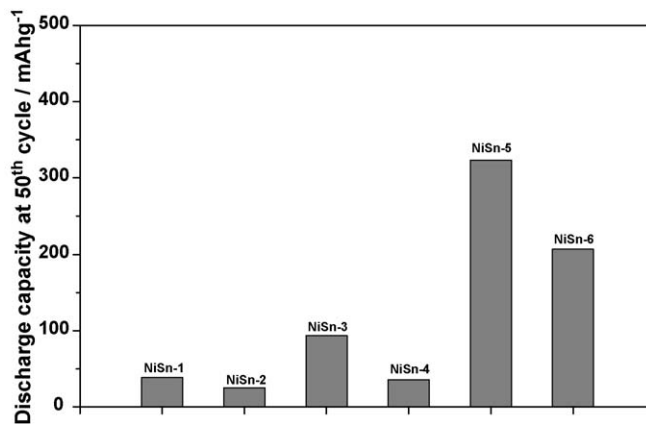

Fig. 5. Voltage profiles at the 10th cycle of lithium cells using samples NiSn-1, NiSn-2, NiSn-3, NiSn-4, NiSn-5 and NiSn-6, respectively, as cathode. EC:DMC 1:1 LiPF$_6$ electrolyte. Charge–discharge current density: 1 A cm^{-2} g^{-1}, about 0.8C rate. Room temperature. For samples' identification see Table 1.

Fig. 6. Discharge capacity at the 50th cycle of cells using different Ni$_3$Sn$_4$ electrodes. Lithium counter electrode. Room temperature. For samples' identification see Table 1.
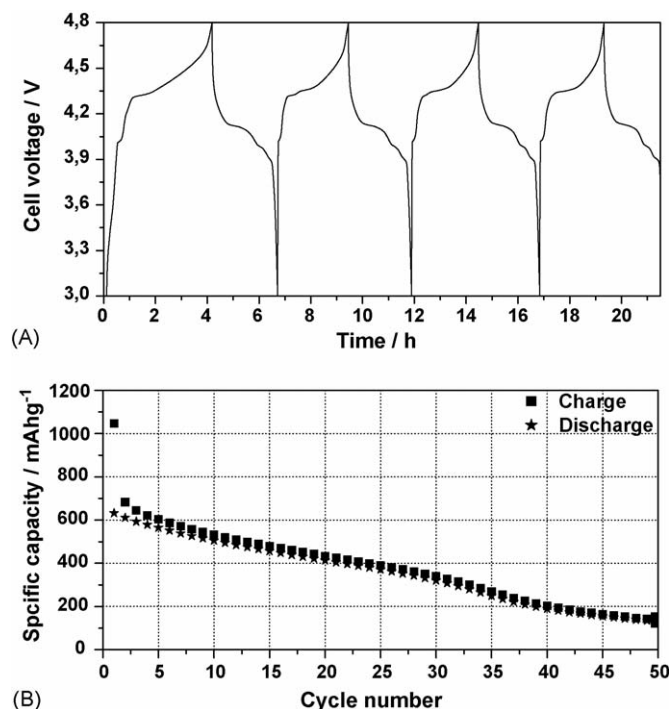
Fig. 7. Voltage–time profiles of typical charge–discharge cycles (A) and capacity delivered upon cycling of a NiSn-5/EC:DMC 1:1 LiPF$_6$/LiNi$_{0.5}$Mn$_{1.5}$O$_4$ lithium ion cell. Charge–discharge current density: 0.5 A cm^{-2} g^{-1}, about C/2.5 rate. Room temperature.

show that the best cycling behaviour is obtained with samples where the metastable phase predominated, i.e. samples NiSn-3, NiSn-5 and, particularly, sample NiSn-5.

Although this work was mainly devoted to the investigation of the conditions of the electrodeposition process, the results have encouraged us to test in a preliminary way sample NiSn-5 as anode in a complete lithium ion cell using a high voltage, nickel manganese spinel, LiNi$_{0.5}$Mn$_{1.5}$O$_4$ as cathode and a typical EC:DMC LiPF$_6$ solution as electrolyte. The steady state electrochemical process of this cell is assumed to be:

$$x\mathrm{LiNi_{0.5}Mn_{1.5}O_4} + \mathrm{Sn} \underset{\text{discharge}}{\overset{\text{charge}}{\rightleftarrows}} \mathrm{Li}_x\mathrm{Sn} + \mathrm{Li}_{(1-x)}\mathrm{Ni_{0.5}Mn_{1.5}O_4}$$
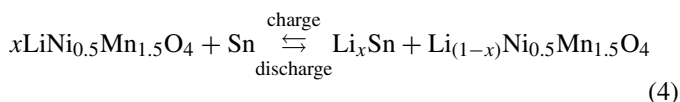
$$(4)$$

Fig. 7A shows the voltage profile of some typical charge–discharge cycles of the cell while Fig. 7B illustrates the capacity (referred to the anode) delivered upon cycling. The cell operates around 4.0 V with a good charge–discharge efficiency and with a very high reversible capacity, i.e. around 550 mA hg^{-1} at a reasonable C/2.5 rate. Some decay in capacity is observed upon cycling, this probably being due to a not yet optimized morphology of the intermetallic electrode, as well as to a not properly balanced cell structure. Although further work is certainly required to refine the cell structure and to improve its performance, these preliminary results are quite promising in confirming the validity of the optimized Ni$_x$Sn$_y$ intermetallic as an effective anode to be used in alternative to graphite in new types of lithium ion batteries.

4. Conclusion

As expected, the right type morphology and of the phase are crucial parameters for assuring a proper operation of intermetallic electrodes, obviously with specific differences depending on the various materials considered. This has been clearly demonstrated in this work where, by choosing a synthesis methods which allows to control and monitor the final electrode structure, it has been shown that the electrochemical performance of Ni$_3$Sn$_4$ electrodes varies consistently just slightly varying their morphology. The best performance has been obtained with sample NiSn-5 which has a morphology based on pillars formed by a regular agglomeration of low particle size grains and which assumes a predominant metastable phase. Minor changes, such as those involving a slightly more disordered morphology and a growth in particle size, result in a consistent decay in capacity delivery.

However, although the selected sample NiSn-5 has a good specific capacity, i.e. of the order of 550 mA hg^{-1} and may be successfully used as a cathode in a complete lithium ion cell, its performance is not yet fully satisfactory, especially in terms of stability and cycle life. Indeed, Fig. 4 shows that the capacity delivery of this sample starts to decay after the 40th cycle, this demonstrating that its configuration has still to be improved. On the other hand, the fact that even under these not fully optimized conditions, the capacity values of the NiSn-5 based cell largely exceed those reported in the literature for similar cells [7,8,13], allows us to assume that the approach described in this work, i.e. a controlled electrodeposition synthesis, may be the right tool to reach this goal. For instance, this may be attempted by further varying the current regimes and/or, particularly, the type of substrate. This will be verified in our laboratory and the results will be reported in future papers.

Acknowledgements

References

[1] J. Yang, Y. Takeda, N. Imanischi, J.Y. Xie, O. Yamamoto, Solid State Ionics 133 (2000) 189.
[2] D. Larcher, L.Y. Beaulieu, O. Mao, A.E. George, J.R. Dahn, J. Electrochem. Soc. 147 (2000) 1703.
[3] R. Benedek, M.M. Thackeray, J. Power Sources 110 (2002) 406.
[4] C.S. Johnson, J.T. Vaughey, M.M. Thackeray, T. Sarakonsri, S.A. Hackney, L. Fransson, K. Edström, J.O. Thomas, Electrochem. Commun. 2 (2002) 595–600.
[5] Z. Chen, V. Chevrier, L. Christensen, J.R. Dahn, Electrochem. Solid State Lett. 7 (2004) A310.
[6] M. Winter, J.O. Besenhard, Electrochim. Acta 45 (1999) 31.
[7] H.-Y. Lee, S.-W. Jang, S.-M. Lee, S.-J. Lee, H.-K. Baik, J. Power Sources 112 (2002) 8.

[8] H. Mukaibo, T. Sumi, T. Yokoshima, T. Momma, T. Osaka, Electrochem. Solid State Lett. 6 (2003) A218.

[9] Q.F. Dong, C.Z. Wu, M.G. Jin, Z.C. Huang, M.S. Zheng, J.K. You, Z.G. Lin, Solid State Ionics 167 (2004) 49.

[10] I. Amadei, S. Panero, B. Scrosati, G. Cocco, L. Schiffini, J. Power Sources 143 (2005) 227.

[11] H. Mukaibo, T. Osaka, P. Reale, S. Panero, B. Scrosati, M. Wacthler, J. Power Sources 132 (2004) 225.

[12] T. Watanabe, T. Hirose, K. Arai, M. Chikazawa, J. Jpn. Inst. Met. 63 (1999) 496.

[13] X.-Q. Cheng, P.-F. Shi, J. Alloys Compd. 391 (2005) 241.